NSF GRANT # 0530759
NSF PROGRAM NAME: NEESR

Erosion and Liquefaction Failure of Coastal Sandy Slopes Caused by Breaking Solitary Wave Runup and Drawdown

Yin Lu (Julie) Young
Assistant Professor, Princeton University

Heng Xiao
Graduate Student, Princeton University

Abstract: The objective of this work is to advance the fundamental understanding of soil erosion and liquefaction failure mechanisms caused by breaking solitary wave runup and drawdown. A series of experimental studies were carried out at the NEES@OSU tsunami wave basin. The results showed that breaking solitary waves over a sloping fine sand beach led to net erosion of the shore face and the beach, net deposition in a small region near the maximum excursion point, and net deposition in the wave breaking zone. The physical mechanisms responsible for the sediment entrainment, transport, and deposition have been identified. A comprehensive numerical model was developed to predict near-shore wave propagation, sediment transport, morphological change, and subsurface pore pressure variations. The numerical predictions compared well with experimental measurements. Numerical models were also used to investigate the susceptibility of coastal fine sand slopes to liquefaction failure caused by breaking solitary wave runup and drawdown. The results showed that the soil near the bed surface, particularly along the seepage face, is at risk to liquefaction failure. The risk increases for steeper slopes because of the faster loading and unloading caused by the wave runup and drawdown. The analysis showed that the results are strongly influenced by the soil permeability, relative compressibility between the pore fluids and solid skeleton, as well as nonlinear soil constitutive behavior.

1. Introduction: As demonstrated by the 2004 Indian Ocean Tsunami, extreme wave runup and drawdown can mobilize substantial amount of sediments, the resulting erosion and scour damage can lead to significant morphological changes in coastal regions, and undermine coastal infrastructures (building foundations, roadways, embankments, underground pipelines, etc). In severe cases, liquefaction and slope instability failure may also develop.

In the past, most experimental and numerical modeling of tsunamis focused on wave propagation and inundation, but few studies considered the effect of the mobile bed, and even fewer studies examined the effect of wave-seabed interactions in the near-shore region. Hence, the objectives of this work are to:

(1) investigate the physical mechanisms that influence tsunami erosion and deposition in the littoral zone via physical simulations, and provide experimental data for validation of numerical models,
(2) develop and validate a comprehensive numerical model to predict the transient wave propagation, sediment transport, morphological change, and bed responses in the near-shore region caused by breaking solitary waves, and
(3) use the numerical model to assess the potential for tsunami-induced liquefaction failure of coastal sandy slopes.

2. Physical Simulations of Breaking Solitary Wave Over a Sloping Fine Sand Beach: In order to examine the mechanisms that influence tsunami erosion and deposition, a series of large-scale experiments were carried out in a 48.8 m by 2.16 m by 2.1 m wave flume especially constructed for this project inside the Tsunami Wave Basin at Oregon Stage University (a NEES site). The flume was heavily instrumented to observe free surface elevations, cross-shore water velocities, suspended sediment concentrations, vertical and cross-shore pore pressure gradients near the shoreline, and bed profile changes. In addition, wave-sediment interactions were observed via underwater video cameras. A schematic of the wave flume, bed configuration, and some of the instruments are shown in Fig. 1. Due to space limitations we only present the highlights of the work and a summary of the results here. Details about the setup of the experiments and a complete analysis of the results are presented in [1, 2].

To investigate different approaches of representing tsunamis in reality, solitary and cnoidal waves of different heights were generated. Various bed configurations were studied including 1:15 slope and 1:10 slope, with and without a flat reef and structures,

to represent the wide variety of coastal bathymetries. Here we focus on the results for 60 cm solitary waves (ST60). The time series measured by the wave gauges deployed at different cross-shore locations (see Fig. 1) are presented in Fig. 2.

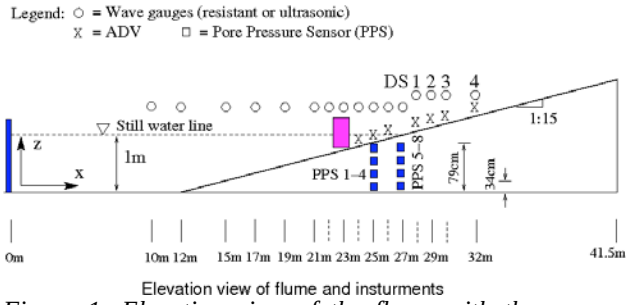

Figure 1: Elevation view of the flume with the wave maker at the left end, sand bed at the right end (with 1:15 bed shown as an example), and some of the instruments. Wave gages (circles) are numbered from 1 (left) to 12 (right). ADV: acoustic Doppler velocimeter; PPS: pore pressure sensor; DS: distance sonic.

From Fig. 2, it can be seen that a plunging breaker initiated immediately after x = 22 m at approximately t = 7.5 sec. After the wave broke, a bore with a height of 20 cm formed at approximately x = 26 m, which then climbed onshore. The wave reached its maximum runup at x = 38.5 m at approximately t = 13 sec, which was followed immediately by wave drawdown. The drawdown wave reached the position of the initial shoreline at around t = 15 sec, leading to a hydraulic jump.

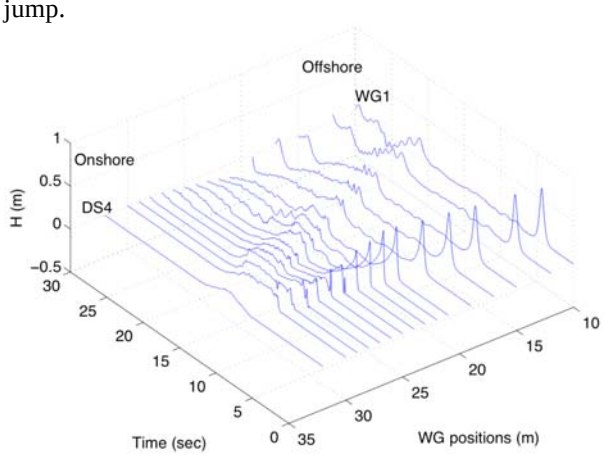

Fig. 2: Water surface elevations measured by wave gauges (1-12 from offshore to onshore direction) and distance sonic sensors (1 to 4 from offshore to onshore direction).

The plunging breaker rebounded from the shallow water near the shoreline and formed a water jet that impinged on the sandy beach at x = 24 to 25 m, entraining large amounts of sand. The sand was then pushed up the slope, a small portion of which was deposited near the tip of the maximum runup (x = 38.5 m) where the water depth and velocity are both very small. Most of the entrained sand was carried back offshore by a rapid, shallow, sheet flow, which resulted in net erosion of the shore face and the beach. The erosion in this region may have also been enhanced by upward seepage force on the sand particles caused by pore pressure gradients. The seaward sheet flow was forced to decelerate when it collided with the large water mass at sea, which formed a hydraulic jump and a large recirculation zone between x = 22 m and x = 24 m. The reduced velocity and the long particle residence time in the recirculation zone allowed time for majority of the entrained sediments to deposit in this region, which coincided with the wave breaking zone. Figure 3 shows the initial bed profile on which ST60 waves were run as well as the bed profiles after three, six, and nine ST60 waves. The starting bed profile corresponds to an initially constant 1:15 slope modified by about 100 solitary waves of smaller sizes. The bed profile changes caused by the waves are shown in Fig. 4. Net deposition is observed in the wave-breaking zone (and also the recirculation zone) and near the tip of the maximum runup. Net erosion is observed on the shore face and on the beach.

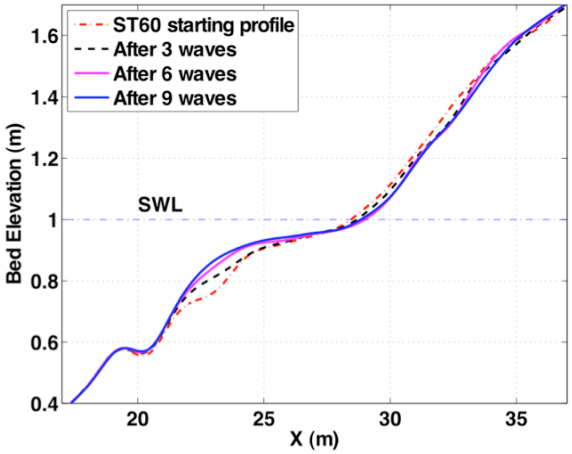

Fig. 3. Measured profiles after three, six, and nine ST60 waves. The bed profile immediately prior to the ST60 wave runs is also shown.

3. Numerical Modeling of Wave Propagation, Sediment Transport, and Morphological Changes:

To complement the experimental studies as presented in Section 2, a comprehensive numerical model was developed to predict the transient wave propagation, sediment transport, bed profile change, and the seabed responses caused by breaking solitary waves runup and drawdown over a sloping beach. The components of the numerical model have been extensively validated against previous analytical, numerical, and

experimental results [3]. The validated numerical model is used to simulate the breaking solitary wave runup and drawdown shown in Section 2. A summary of the numerical model and the comparison with the experimental results are given below.

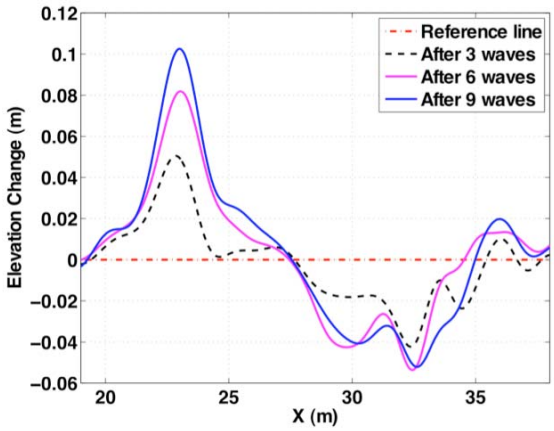

Fig. 4: Measured bed profile changes after three, six, and nine ST60 waves. The line $\Delta z = 0$ is drawn as the reference line.

A depth-averaged Boussinesq equation [4] is adopted to model the wave propagation before the wave breaking in order to accommodate the dispersion effects which are important when the wave is propagating from a distance far away from the shoreline. After the wave broke, the dispersion terms are turned off and the Nonlinear Shallow Water Equation (NSWE) solver is used. The scalar transport equation is used to describe the sediment transport in the water. The erosion and deposition flux is modeled as functions of the local fluid field quantities such as Shields parameter, near-bed sediment concentration, particle settling velocity, and particle Reynolds number. The fluid conservation equations, sediment transport equation, and bed evolution equation are solved simultaneously in the numerical model. All the bed profile changes are assumed to be caused by wave-induced sediment transport, and thus the bed evolves solely due to erosion and deposition.

A finite volume method is used to solve the system of equations describing the wave-sediment interactions. A second order Godonov-type scheme with shock capturing weighted averaged flux is used [5]. To track the location of the shoreline, an exact Riemann solver is used at the dry-wet interface. Details of the numerical model and validation studies are presented in Ref. [3].

The numerical predictions compared well with experimental measurements, as demonstrated in the comparison of the wave-elevation time history in Fig. 5. The arrival time and key features of the wave up to t = 25 sec was captured with good accuracy by the numerical model. For t > 25 sec, wave-wave interactions dominate, which cannot be properly captured by a depth-averaged model (NSWE or Boussinesq), and thus some discrepancies can be observed. The overall agreement is, however, satisfactory. The flow velocity at x = 23 m is compared and presented in Fig. 6. Again, excellent agreements are observed before t = 25 sec, after which wave-wave interaction dominated. The predicted and measured bed profile changes caused by three consecutive ST60 waves are compared in Fig. 7. The locations of the erosion and deposition regions are correctly predicted. The results suggest that the depth-averaged model developed for this project is capable of predicting the wave runup and drawdown, as well as associated sediment transport and morphological changes.

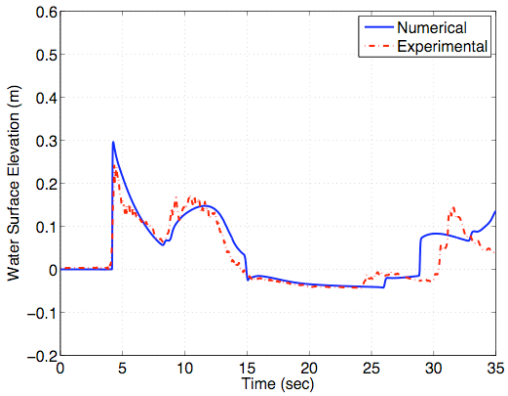

Fig. 6: Numerical simulation and experimental measurements of time series of water surface elevation at x = 27 m (WG12; nominal shoreline).

4. Numerical Modeling of Transient Bed Responses:
The soil skeleton and the pore fluids in the sediment bed are modeled in the framework of poromechanics theory [6]. The soil deposit is assumed to be fully saturated (with either water or air). The governing equations are solved with a finite element code DYNAFLOW [7]. The technical details of DYNAFLOW can be found in [8], where various validation cases were also presented.

Comparisons of the predicted and measured pore pressure changes at the four pore pressure sensors buried in the sand-bed at x = 27 m are shown in Fig. 8. The agreement was satisfactory in general. The observed discrepancy can be attributed to unavoidable spatial variations of soil properties and difficulties in obtaining the in situ sediment/soil properties.

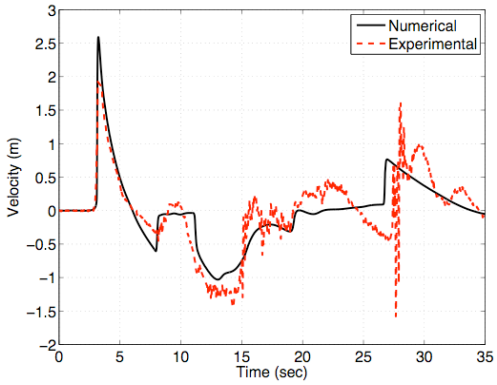

Fig. 6: Numerical simulation and experimental measurements of time series of flow velocity at x = 23 m.

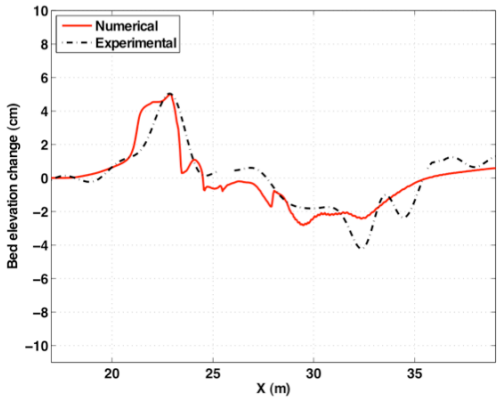

Fig. 7: Changes in bed profile caused by three consecutive 60-cm solitary waves over a nominally 1:15 beach (with 15 minutes settling time between the waves).

5. Numerical investigation of the Liquefaction Potential of Coastal Sandy Slopes Caused by Breaking Solitary Waves: Tsunami runup and drawdown can cause liquefaction failure of coastal fine sand slopes due to the generation of high excess pore pressure and the reduction of the effective over burden pressure during the drawdown. The region immediately seaward of the initial shoreline is the most susceptible to liquefaction failure because the water level drops significantly below the still water level during the set down phase of the drawdown. Along the seepage face between the initial shoreline and maximum drawdown, the subsurface pore pressure cannot drain as fast as bed surface pressure. The sand liquefies when the excess pore pressure exceeds the effective overburden pressure, which is reduced significantly because of the drop in water level.

To access the liquefaction potential in reality, numerical results are presented for the case of a 10-m high solitary wave propagating from an initial water depth of 20 m toward a sloping fine sand beach. Two slopes of 1:15 and 1:5 were considered. The wave propagation, breaking, runup and drawdown, as well as resulting pressure distribution acting on the slope, are computed by solving for the hybrid Boussinesq – nonlinear shallow water equations using the finite volume method. The subsurface excess pore water pressure and deformation fields are solved simultaneously using a stabilized finite element method [9]. Two different soil constitutive models have been examined: a linear elastic model and a non-associative Mohr-Coulomb model. To assess the liquefaction potential, the cumulative maximum mean normal effective stress (σ_m) criterion is used, i.e. the sand is assumed to liquefy when σ_m reaches zero. Details of the model setup, validation studies, and result analysis are given in Refs. [10, 11].

Figure 9 presents a spatial picture of the liquefaction zone for the 1:5 and 1:15 slopes near the end of the wave drawdown. The non-associative Mohr-Coulomb elastoplastic material model is used. The high liquefaction potential zone (σ_m=0) corresponds to the black region. The maximum depth of the liquefaction zone was predicted to be 2.8 m for 1:15 slope case and 4.4 m for 1:5 slope case. The simulation showed that the case with the steeper (1:5) slope is more susceptible to liquefaction failure due to the higher hydraulic gradient caused by the faster runup and drawdown. Further details are presented in [10, 11].

6. Conclusions: The objective of this work is to advance the fundamental understanding of soil erosion and liquefaction failure mechanisms caused by breaking solitary wave runup and drawdown. A series of experimental studies were carried out at the NEES@OSU tsunami wave basin to investigate tsunami erosion and deposition mechanisms. A comprehensive numerical model was developed to predict near-shore transient wave propagation, sediment transport, morphological change, and bed responses in the near-shore region. The numerical model was validated by comparing the results with experimental measurements. To assess the liquefaction potential of coastal fine sand slopes, full-scale simulations were carried out using the numerical model. The results demonstrated that the soil near the bed surface along the seepage face is at risk to liquefaction failure, and the risk increases for increasing slope. Details of related findings can be found in [1-3,10-16].

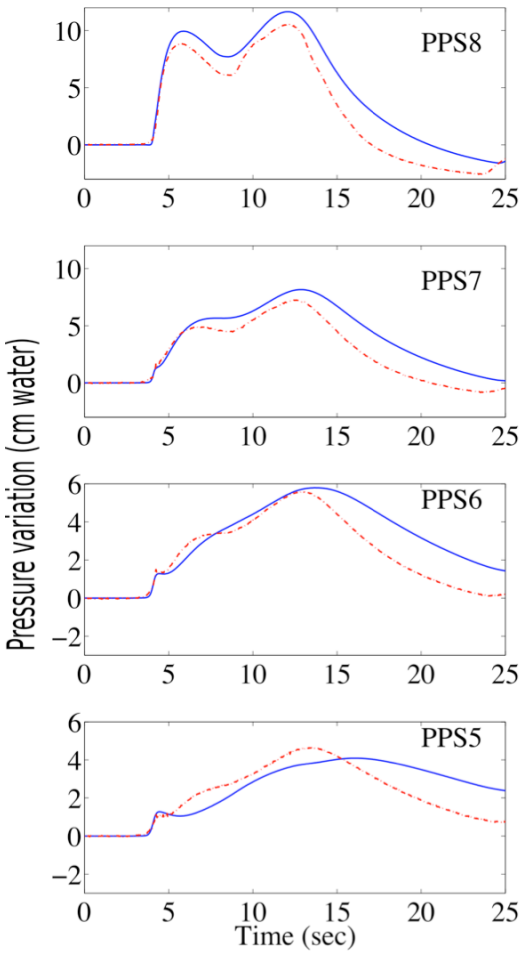

Fig. 8: Time history of pore pressure variation at PPS5-8 (located at x = 27 m; co-located with WG12).

7. Future Work: It should be noted that only a small portion of the experimental data from the tsunami scour study has been analyzed. Additional work is underway to study the influence of bathymetry (constant slope vs. reef-type bathymetry), waveform (cnoidal vs. solitary wave), and coastal structure (large cylindrical pier) on wave runup and drawdown characteristics, sediment erosion and deposition mechanisms, and bed responses. Additional work is underway to model the transient response of the vadose and the phreatic zones subject to extreme wave loads, including the effects of relative compressibility between the constituents (air, water, and soil skeleton) and saturation front propagation [17]. Finally, additional work is also needed to model potential slope instability failure caused by tsunami runup and drawdown.

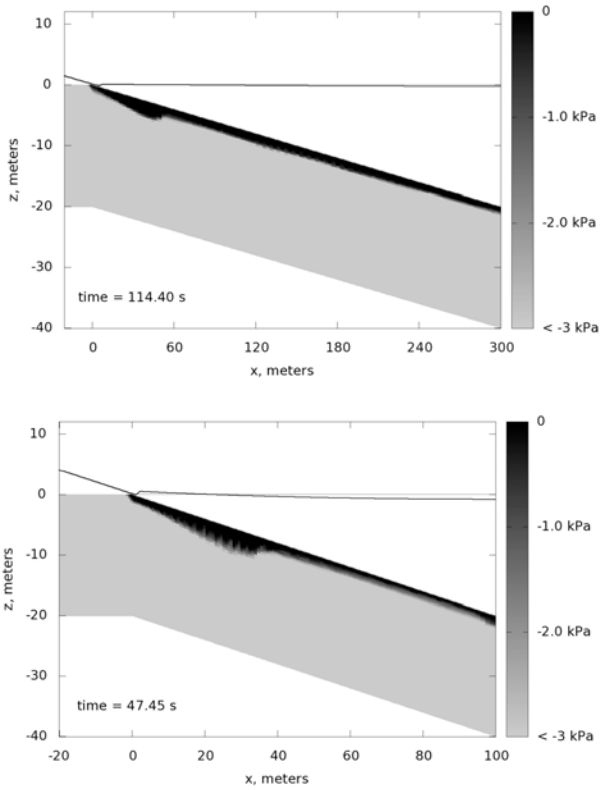

Fig. 9: Contour of the maximum mean normal stress in the 1:15 slope (top) and 1:5 slope (bottom) after the runup and drawdown. The high liquefaction potential zone corresponds to the black region.

8. Acknowledgements: The authors would like to acknowledge funding by the National Science Foundation through the NSF George E. Brown, Jr. Network for Earthquake Engineering Simulation (grant no. 0530759) and through the NSF CMMI grant no. 0653772. The authors would also like to acknowledge the contribution of Prof. Ronald Borja and Mr. Josh White from Stanford University, and Prof. Jean Prevost from Princeton University.

9. References:

[1] Y.L. Young, H. Xiao & T. Maddux, Runup and drawdown of breaking solitary waves over sand beach. Part I: Experimental Modeling, Submitted to Marine Geology, 2008.

[2] H. Xiao and Y.L. Young, Solitary Wave Runup on Movable Bed: Experimental and Numerical Investigations, NEES 6TH Annual Meeting: The Value of Earthquake Engineering Research, Portland, OR, June 18-20, 2008.

[3] H. Xiao, Y.L. Young, & J.H. Prevost, Runup and drawdown of breaking solitary waves over sand beach. Part II: Numerical Simulation. Submitted to Marine Geology, 2008.

[4] P.A. Madsen, R. Murray, O.R. Sørensen,. A new form of the Boussinesq equations with improved linear dispersion characteristics. Part I. Coastal Engineering vol. 15 (4), pp 371–388, 1991.
[5] E. Toro, Shock-Capturing Methods for Free-Surface Shallow Flows. John Wiley & Sons, Ltd, 2000
[6] O. Coussy, Poromecahnics. John & Wiley, Hoboken, NJ, 2004.
[7] J.H. Prevost, DYNAFLOW: A nonlinear transient finite element analysis programme. Dept. of Civil Engineering, Princeton University, Princeton, NJ, (last updated 2008), 1983.
[8] J.H. Prevost, Implicit-explicit schemes for nonlinear consolidation. Comp. Meth. Appl. Mech. Engrg. vol. 39, pp 225–239, 1983.
[9] White J, Borja R (2008) Stabilized low-order finite elements for coupled solid-deformation/fluid-diffusion and their application to fault zone transients. Comput. Methods Appl. Mech. Eng. vol. 197:49-50, pp 4353-4366, 2008.
[10] Y.L. Young, J. White, H. Xiao, and R.I. Borja, Tsunami-induced Liquefaction Failure of Coastal Slopes, Acta Geotechnica, vol 4 (1), pp.17-32, 2009.
[11] Y.L. Young, H. Xiao, J. White, & R.I. Borja, Can Tsunami Lead to Liquefaction Failure of Coastal Sandy Slopes, 14th World Conf. on Earthquake Engrg., Beijing, China, Oct. 12-17, 2008.
[12] Y.L. Young & H. Xiao, Enhanced Sediment Transport due to Wave-Soil Interactions, Proc. NSF Engineering Research and Innovation Conference, Knoxville, TE, Jan. 8-10, 2008.
[13] H.R. Riggs, I.N. Robertson, K.F. Cheung, G. Pawlak, Y.L. Young, and S. Yim, Experimental Simulation of Tsunami Hazards to Buildings and Bridges, Proceedings of NSF Engineering Research and Innovation Conference, Knoxville, TE, January 8-10, 2008.
[14] I.N. Robertson, S. Yim, H.R. Riggs, and Y.L. Young, Coastal Bridge Performance During Hurricane Katrina, 3rd International Conference on Structural Engineering, Mechanics and Computation, Cape Town, South Africa, Sept. 9-12, 2007.
[15] H. Xiao and Y.L. Young, Modeling of Solitary Waves over a Movable Bed, 9th US National Congress on Computational Mechanics, San Francisco, CA, July 23-26, 2007.
[16] Y.L. Young and H. Xiao, Numerical and Experimental Investigations of Tsunami-Induced Sediment Transport, American Geophysics Union 2007 Joint Assembly, Acapulco, Mexico, May 22-25, 2007.
[17] Y.L. Young, J.H. Prevost, J.A. Smith, H. Xiao, S. Sanborn, M.L Beack, and N. Lin, Numerical Modeling of Hurricanes and Storm Surges, Near-shore Wave-Soil Interactions, and Slope Instability Failures, Proc. 2009 NSF Engineering Research and Innovation Conference, Honolulu, Hawaii, 2009.